Eur. Phys. J. D **32**, 271–276 (2005)
DOI: 10.1140/epjd/e2005-00012-2

THE EUROPEAN PHYSICAL JOURNAL D

Three-step laser excitation of the $6p_{3/2}ns$, nd, ng autoionizing Rydberg levels via the $6p5f\ 1/2[5/2]_2$ level of lead

A. Ahad[1], A. Nadeem[1], S.A. Bhatti[2], and M.A. Baig[1,a]

[1] Atomic and Molecular Physics Laboratory, Department of Physics, Quaid-i-Azam University, Islamabad 45320, Pakistan
[2] Applied Physics Division, PINSTECH, PO Nilore, Islamabad, Pakistan

Received 28 February 2004 / Received in final form 13 August 2004
Published online 1st February 2005 –

Abstract. Odd parity autoionizing Rydberg levels of atomic lead in the energy region above the $6p_{1/2}$ ionization threshold have been investigated using three-step laser excitation in conjunction with an atomic beam apparatus. The $6p_{3/2}ns$ $(J = 1, 2)$, $6p_{3/2}nd$ $(J = 1, 2, 3)$ and $6p_{3/2}ng$ $(J = 2, 3)$ levels have been observed from the $6p5f\ 1/2[5/2]_2$ intermediate level. Energy values and FWHM of forty levels belonging to the $6p_{3/2}ns$, $6p_{3/2}nd$ and $6p_{3/2}ng$ configurations are presented. Six levels based on the $6p_{3/2}ng$ (5, $13 \leq n \leq 15$) configurations and three levels attached to the $6p_{3/2}8d$ configuration are reported for the first time. The present study of the low-lying autoionizing levels attached to the $6p_{3/2}5g$ $(J = 2, 3)$ configuration completes the series adjacent to the $6p_{1/2}$ limit.

PACS. 32.30.-r Atomic spectra – 32.30.Jc Visible and ultraviolet spectra – 32.80.Rm Multiphoton ionization and excitation to highly excited states (e.g., Rydberg states)

1 Introduction

Lead belongs to the fourth group atoms of the Periodic Table and possesses p^2 configuration in the ground state. Its spectra have been extensively studied using conventional as well as laser spectroscopic techniques. The photo-absorption spectra of lead was studied by Garton and Wilson [1] using a 3 m spectrograph equipped with a 1200 lines per mm grating and observed the $6p_{1/2}ns$ $(8 \leq n \leq 32)$ and $6p_{1/2}nd$ $(6 \leq n \leq 53)$ $J = 1$ odd parity levels converging on the $6p_{1/2}$ limit. In addition, three $J = 1$ autoionizing series converging on the $6p_{3/2}$ limit were recorded covering the spectral region from 110 to 220 nm. Wood and Andrew [2] studied the emission spectrum of lead using an electrode less discharge tube containing halides of lead. In the spectral region from 197.7 nm to 1256.1 nm 370 lines were measured and classified, 59 lines as even parity and 58 as odd parity levels. Much of the early data have been tabulated in the NBS table [3].

Brown et al. [4] photographed the absorption spectrum of lead in the region from 135 to 204 nm using a 6.6 m spectrograph and reported the $6pns$ and $6pnd$ $J \leq 2$ levels excited from the $6p^2\ (1/2, 1/2)_0$ ground level in addition to thermally populated $6p^2\ (3/2, 1/2)_1$ and $(3/2, 1/2)_2$ levels. Beside the discrete energy region, the region between the first and the second ionization limit was also explored. An improved values for the first and second ionization limits of lead were determined as 59 819.57(10) cm^{-1} and 73 900.64(10) cm^{-1} respectively. Subsequently, Connerade et al. [5] extended the observed spectra to higher energies and reported the $6s6p^2\ (1/2, 3/2, 1/2)_{1/2}\ np[1/2, 3/2]_1$ series $(7 \leq n \leq 15)$ converging to $6s6p^2\ (1/2, 3/2, 1/2)_{1/2}$ limit at 117 731 cm^{-1}, $6s6p^2\ (1/2, 1/2, 1/2)_{1/2}\ np[1/2, 3/2]_1$ series for $(7 \leq n \leq 21)$ converging to the $6s6p^2\ (1/2, 1/2, 1/2)_{1/2}$ limit at 148 068 cm^{-1} and $6s6p^2\ (1/2, 3/2, 3/2)_{1/2}\ np[1/2, 3/2]_1$ series $(9 \leq n \leq 15)$ converging to the $6s6p^2\ (1/2, 3/2, 3/2)_{1/2}$ limit at 164 117 cm^{-1}. In addition, the $5d^96s^26p^2\ (3/2, 1/2, 1/2)_{3/2}\ np$, nf $J = 1$ series $(7 \leq n \leq 15)$ converging to the $5d^96s^26p^2\ (3/2, 1/2, 1/2)_{3/2}$ limit were also observed.

Using the step-wise laser excitation spectroscopic technique, Bolshov et al. [6] excited the $6p7s\ (1/2, 1/2)_1$ resonance level of lead and registered the fluorescence spectra. Buch et al. [7] prepared an atomic beam in the $6p^2\ (3/2, 3/2)_2$ metastable state by a discharge and used the second harmonic of a CW dye laser to study the $6p_{1/2}\ n\ell$ $(16 \leq n \leq 67)$, $\ell = 0, 2, 4$, $J = 1, 2, 3$ odd parity Rydberg levels converging on the first ionization limit. Young et al. [8] used a pulsed dye laser to dissociate the lead dimmers via two-photon photodissociation mechanism that left lead atoms in the $6p7s\ (1/2, 1/2)_1$ excited state and the $6p^2\ (1/2, 1/2)_0$ ground state. A third photon from the same laser pulse took the atoms from the $6p7s\ (1/2, 1/2)_1$ excited state to the

[a] e-mail: baig@qau.edu.pk

$6pnp$ $(1/2,3/2)_{2,1}$, $6pnp$ $(1/2,1/2)_0$ and $6pnf$ $(1/2,5/2)_2$ even parity Rydberg states. Ding et al. [9] studied the even parity $J = 0, 2$ Rydberg levels of lead using the two photons excitation scheme. Dembeyznski et al. [10] observed the odd parity levels of lead and determined an improved value of the first ionization potential as 59 819.558 cm^{-1}. Recently, Farooqi et al. [11] used the two-step laser excitation scheme and observed the even parity $6pnp$ $(1/2,3/2)_{2,1}$, $6pnp$ $(1/2,1/2)_0$, and $6pnf$ $(1/2,5/2)_2$ Rydberg states. Hasegawa and Suzuki [12] also reported the $6pnp$ $(1/2,3/2)_{2,1}$, $6pnp$ $(1/2,1/2)_0$, and $6pnf$ $(1/2,5/2)_2$ even parity levels using the multi-step laser excitation scheme.

More recently, Bhatti et al. [13] observed and assigned more than 200 levels of the $6p_{3/2}ns$ $(J = 1, 2)$, $6p_{3/2}nd$ $(J = 0, 1, 2, 3)$ odd parity autoionizing Rydberg series near the $6p_{3/2}$ ionization limit. They populated four different intermediate levels namely $6p_{3/2}7p$ $J = 1, 2$ to reach the highly excited levels using the three-step laser excitation and made a consistent assignments to the observed Rydberg series. Nawaz et al. [14] excited the $6p_{3/2}ns$ $(J = 1, 2)$, $6p_{3/2}nd$ $(J = 1, 2, 3)$ series via the $6p7f$ $(J = 2)$ and $6p8f$ $(J = 2)$ intermediate levels. They reported forty new levels on the lower energy side. An interesting observation was made that the observed spectra excited via $6p8f$ $1/2[5/2]_2$ and $6p7f$ $1/2[5/2]_2$ routes were similar to those obtained via the $6p7p$ $1/2[5/2]_2$ level, which alluded that the $6p8f$ $1/2[5/2]_2$ and $6p7f$ $1/2[5/2]_2$ levels contain large $6p7p$ $1/2[5/2]_2$ character. In an attempt to excite the $6p_{3/2}ng$ autoionizing levels and to extend the $6p_{3/2}ns$ and $6p_{3/2}nd$ spectra toward the red side, Bhatti et al. [15] employed the $6p6f$ $1/2[5/2]_2$ level as an intermediate step. The $6p6f$ $1/2[5/2]_2$ level at 55 360.078 cm^{-1} (Wood and Andrew [2]), is well isolated in energy from all the $6p_{3/2}7p$ $J = 1, 2$ levels and possesses essentially the f-character. They reported about fifty levels including the $6p_{3/2}ng$ $(6 \leq n \leq 12)$ autoionizing series. The $6p_{3/2}nd$ series was extended down to $n = 9$ and the $6p_{3/2}ns$ down to $n = 11$. The unobserved levels between the first and the second ionization limits that need to be investigated are leading member of the $6p$ $3/2ng$ series $(n = 5)$, two members of the $6p$ $3/2nd$ $(n = 7, 8)$ series and three members of the $6p$ $3/2ns$ $(n = 8, 9, 10)$ series. Fortunately, the $6p5f$ $1/2[5/2]_2$ level at 52 849.801 cm^{-1} [2] can also be used as an intermediate level to access the low lying members of the autoionizing resonances. In the present work it was intended to reach the upper levels via this route to complete the spectra on the lower energy side. In addition, an unexplained phenomenon was reported by Bhatti et al. [15], that the $6pns$ $3/2[3/2]_2$ levels for $(15 \leq n \leq 17)$ did not appear, when excited via the $6p6f$ $1/2[5/2]_2$ intermediate level, although they were very prominent when excited through other routes namely $6p8f$ $1/2[5/2]_2$, $6p7f$ $1/2[5/2]_2$ and $6p7p$ $1/2[5/2]_2$. In order to get more intuition and possible elucidation for this ambiguity the energy region for the higher principal quantum numbers $n \geq 15$ was also scanned. In the present work the $6p_{3/2}ng$ $(5, 11 \leq n \leq 15)$, $6p_{3/2}nd$ $(8, 13 \leq n \leq 18)$ and $6p_{3/2}ns$ $(15 \leq n \leq 20)$ autoionizing levels have been observed which completes the data on the energies and widths of the levels in between the first and second ionization limits of lead.

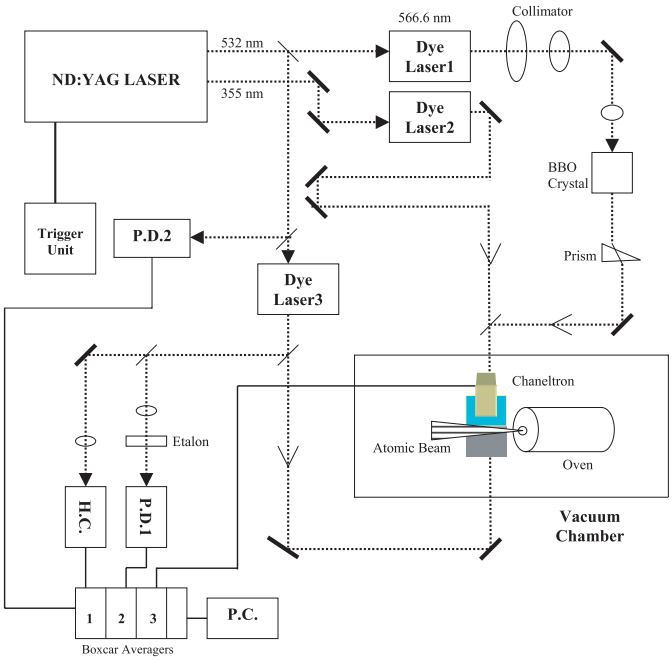

Fig. 1. A Schematic diagram of the experimental set-up. P.D.1: photodiode 1, P.D.2: photodiode 2, H.C.: hollow cathode lamp.

2 Experimental set-up

The schematic diagram of the experimental set-up is shown in Figure 1. Three dye lasers were simultaneously pumped by a common Nd: YAG (Spectra Physics) laser. The dye lasers were Hansch version [16], modified by Hanna [17]. In these dye lasers, a prism was used as a beam expander, instead of a telescope. A 100% mirror replaced the output coupler, which was a 5% reflection window in the original Hansch laser, and the output of the laser was the reflection from the prism. This prism expands the fluorescence from the dye cell so that it covers the entire diffraction grating for higher resolution and narrow laser line width. The holographic grating used in these dye lasers has 3000 lines/mm. The best line width so far achieved was $\leq$0.3 cm^{-1}. The grating was mounted on a precision rotation stage. To tune the dye laser for the desired wavelength, a stepper motor drives the rotation stage of the dye laser that covers about 0.05 cm^{-1} in a single step.

All the three dye lasers were tuned according to the excitation scheme shown in Figure 2. A beam of the neutral lead atoms at low pressure was prepared in an atomic beam apparatus. The apparatus consists of an oven, two aluminum plates and a channeltron, enclosed in a cylindrical vacuum chamber. In the oven a tantalum crucible was heated by passing high current through a 0.05 mm thick tantalum foil wrapped around but without any contact with the crucible. About 3 grams of

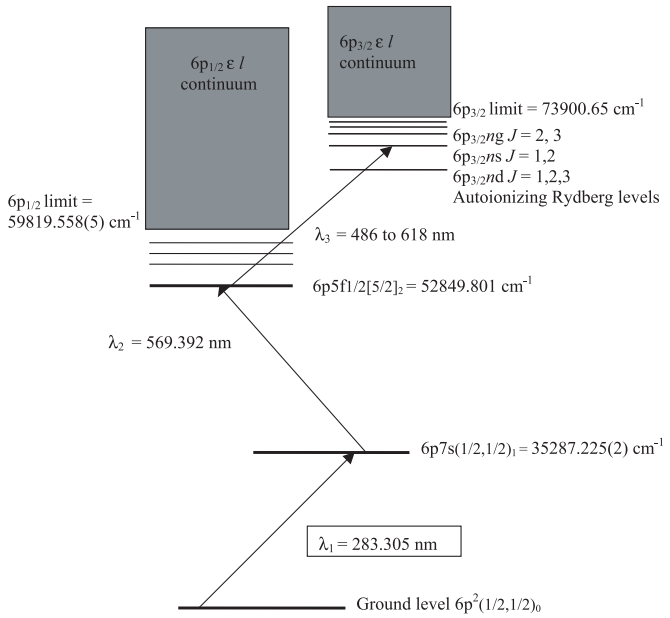

Fig. 2. Three-step laser excitation scheme of the odd-parity autoionizing levels via the $6p5f\ 1/2[5/2]_2$ intermediate level of lead.

lead ingots were placed in the crucible and a current of 100–140 A was passed across the tantalum foil surrounding the crucible. The working temperature for lead was about 1000 K at which the atomic density in the interaction region was about 10^{12} atoms/cm^3. Inside the chamber, two 50×50 mm^2 aluminum plates separated by 10 mm were mounted. To allow a field free interaction of the atomic beam with lasers, both these plates were grounded. All the three laser beams were spatially overlapped that excited the lead atoms from the ground state to the desired autoionizing levels and the ions generated were detected by the channeltron mounted on the top plate. About 1500 to 2000 volts were applied to the channeltron to get an appropriate multiplication of the ion signal.

The first dye laser tuned at 566.6 nm was frequency doubled by a BBO crystal to populate the $6p7s\ (1/2, 1/2)_1$ level at 35 287.225 cm^{-1} [2]. Since the output of the dye laser was vertically polarized therefore the second harmonic from the BBO crystal was horizontally polarized. The second dye laser was tuned at 569.2 nm to approach the $6p5f\ 1/2[5/2]_2$ level at 52 849.801 cm^{-1}. The second dye laser was delayed by about 6 ns with respect to the first dye laser. Both the first and the second dye lasers were pumped by the second harmonic of the Nd:YAG laser. The third dye laser was also delayed by about 5 ns with respect to the second dye laser and was scanned to cover the energy regions of interest for the present work. At the lower energy side the third laser was swept from 620 to 598 nm and for the higher energy region it was scanned from 504 to 484 nm. In this way we were able to explore the energy regions from 69 000 cm^{-1} to 69 520 cm^{-1} and from 72 730 cm^{-1} to 73 430 cm^{-1}.

In order to calibrate the scanning laser wavelength, a small fraction of the dye laser beam was inserted into a neon filled hollow cathode lamp and another small portion was passed through a 1-mm thick fused silica etalon (FSR 3.333 cm^{-1}). The neon spectrum from the hollow cathode lamp provided well-documented reference lines, whereas, the etalon fringes recorded through a photodiode serve as relative energy markers of the scanning laser. The three independent signals from the channeltron, hollow cathode lamp and the photodiode, after processing by three boxcar averagers (SR250) were saved in a PC through a GPIB interface.

3 Results and discussion

The energy levels diagram of lead showing the pertinent levels excited in the present work is shown in Figure 2. The j_cK coupling scheme has been adopted to designate the energy levels. In this coupling scheme $\{[(\ell_1,\ s_1)j_c,\ \ell_2]K,\ s_2\}_J$, the angular momentum quantum number of the $6p$ core electron is $j_c = 3/2$, the K quantum number is the sum of the j_c and the orbital angular momentum quantum number ℓ_2 of the excited electron. The total angular momentum J, is the vector sum of the K quantum number and the spin quantum number s_2 of the excited electron. The levels are designated as $j_c[K]_J$. Following the dipole selection rules, we expect to observe the $6pns\ 3/2[3/2]_{1,2}$, $6pnd\ 3/2[3/2]_{1,2}$, $6pnd\ 3/2[5/2]_{2,3}$, $6pnd\ 3/2[7/2]_3$, $6png\ 3/2[5/2]_{2,3}$ and $6png\ 3/2[7/2]_3$ autoionizing series excited from the $6p5f\ 1/2[5/2]_2$ intermediate. All these series are attached to the $6p_{3/2}$ ionization limit at 73 900.65 cm^{-1}.

In Figures 3a and 3b we reproduce a section of the spectrum showing the $6p14d$, $6p11g$ and $6p16s$ configurations based levels excited from two different intermediate levels. The top spectrum was recorded using the $6p6f\ 1/2[5/2]_2$ intermediate level (Bhatti et al. [15] whereas the bottom spectrum is recorded using $6p5f\ 1/2[5/2]_2$ as an intermediate level. From the comparison of the two data, it is evident that the spectra are very much the same. Therefore, the level assignments is straight forward and we safely assign the newly observed levels as an extension of the $6p_{3/2}nd$, $6p_{3/2}ng$ and $6p_{3/2}ns$ series observed by Nawaz et al. [14] and Bhatti et al. [15]. The broad structure around 72 980 cm^{-1} is the dominating structure in the figure that has been identified as $6p14d\ 3/2[7/2]_3$. The width of this line FWHM is 10 cm^{-1}. The noise level in the present work seems to be high that may be attributed to the fact that the $6p5f\ 1/2[5/2]_2$ level lies further away from the $6p7p\ 3/2[5/2]_2$ perturbing level and thus possess mainly the f-character. In our previous work, Bhatti et al. [15], due to this noise, our observations were limited up to only 73 220 cm^{-1}. In the present experiment we have managed to register the spectrum up to 73 430 cm^{-1} mainly due to improvement of the dye lasers and closely monitoring the atomic beam. The reference of our earlier work enabled us to differentiate between the genuine lines and noise spikes occasionally appear in the spectrum and seems to be a good spectral line after smoothing.

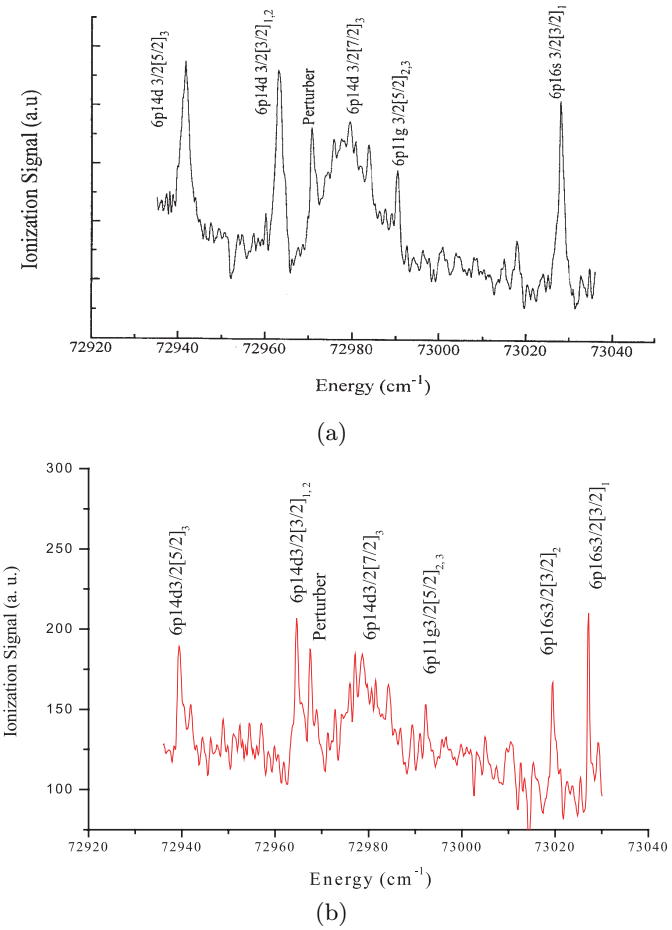

Fig. 3. Autoionizing spectrum of $6p_{3/2}14d$, $6p_{3/2}11g$ and $6p_{3/2}16s$ configurations: (a) excited from the $6p6f\ 1/2[5/2]_2$ intermediate level; (b) excited from the $6p5f\ 1/2[5/2]_2$ intermediate level.

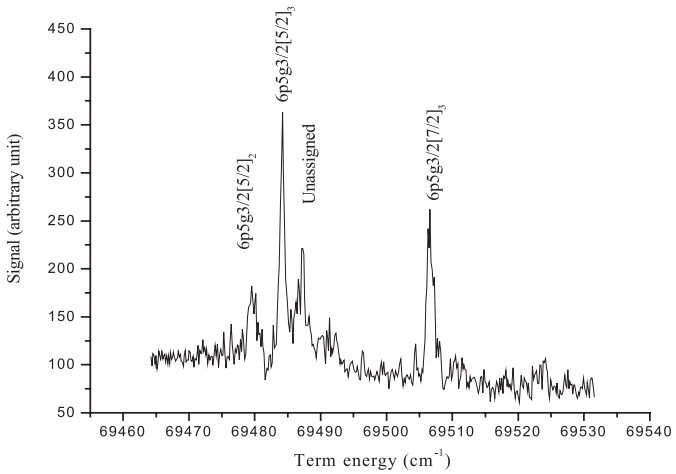

Fig. 4. The lowest autoionizing levels $6p5g\ 3/2[5/2]_{2,3}$ and $6p5g\ 3/2[7/2]_3$ observed via the $6p5f\ 1/2[5/2]_2$ intermediate level.

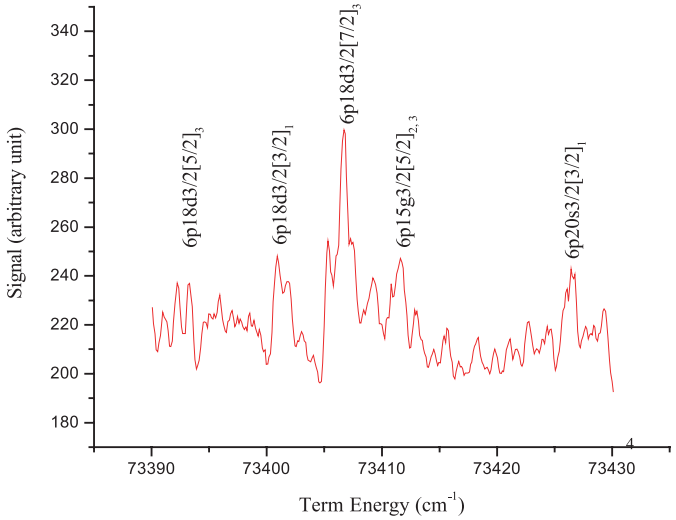

Fig. 5. Autoionizing spectrum covering the energy region from 73 390 cm^{-1} to 73 430 cm^{-1}. It is the last multiplet that has been observed via the $6p5f\ 1/2[5/2]_2$ intermediate level.

Figure 4 shows the lowest levels of the $6p_{3/2}5g$ configuration excited from the $6p5f\ 1/2[5/2]_2$ intermediate level. The spectrum covers the energy region of about 70 cm^{-1} from 69 465 cm^{-1} to 69 535 cm^{-1} and shows the $6p5g\ 3/2[5/2]_{2,3}$ and $6p5g\ 3/2[7/2]_3$ excited levels. The term energies of the $6p5g\ 3/2[5/2]_{2,3}$ doublet are 69 479.53 cm^{-1} and 69 484.20 cm^{-1} and the corresponding effective quantum numbers are 4.982 and 4.985 respectively. The $6p5g\ 3/2[7/2]_3$ level lies at 69 506.62 cm^{-1} with effective quantum number at 4.997. These levels are among those observed for the first time. Since these levels lie far away from the $6p_{3/2}$ ionization limit therefore full multiplicity of the levels have been resolved. The fine structure splitting for the $6p5g\ 3/2[5/2]_{2,3}$ doublet are reported for the first time. A feature observed at 69 487.26 cm^{-1} with effective quantum number 4.986 remains unassigned. On the higher energy region three additional members of the $6png\ 3/2[5/2]_{2,3}$ $(13 \leq n \leq 15)$ series have been observed.

Figure 5 shows the autoionizing spectrum in the energy region from 73 390 to 73 430 cm^{-1} which covers the energy levels based on the $6p_{3/2}18d$, $6p_{3/2}15g$ and $6p_{3/2}20s$ configurations excited from the $6p5f\ 1/2[5/2]_2$ intermediate level. In this energy region the $6pnd\ 3/2[7/2]_3$ lines are more prominent. Although this part of the spectrum is very noisy and it is hard to distinguish between the noise and the true signal, but with the help of our previous studies of the corresponding spectra excited from the $6p6f\ 1/2[5/2]_2$ intermediate level Bhatti et al. [15], the level designations have been made.

The term energies of all the $6p_{3/2}nd$ $(J = 1, 2, 3)$, $(8, 13 \leq n \leq 18)$ autoionizing levels have been calculated as the sum of the frequencies of the first two dye lasers and the transition energy from the third dye laser that are listed in Table 1. The corresponding effective quantum numbers with respect to the $6p_{3/2}$ ionization threshold are calculated using the Rydberg relation

$$E_n = ip - \frac{R_{\mathrm{Pb}}}{(n - \mu_\ell)^2}$$

Sr No	Assignments	Term energy (cm^{-1})	n^*	Γ (cm^{-1})	$\Gamma\ n^{*3}$
1	$6p8d\ 3/2[3/2]_2$	69 141.1	4.802	1.9	2.1×10^2
2	$6p8d\ 3/2[3/2]_1$	69 183.7	4.823	1.1	1.3×10^2
3	$6p8d\ 3/2[7/2]_3$	69 348.6	4.91	5.1	6.0×10^2
4	$6p13d\ 3/2[5/2]_3$	72 736.7	9.71	1.5	1.4×10^3
5	$6p13d\ 3/2[3/2]_1$	72 759.3	9.805	1.2	1.1×10^3
6	$6p14d\ 3/2[5/2]_2$	72 938.8	10.684	0.5	6.6×10^2
7	$6p14d\ 3/2[5/2]_3$	72 941.8	10.698	2.3	2.8×10^3
8	$6p14d\ 3/2[3/2]_1$	72 964.5	10.827	0.5	5.8×10^2
9	$6p14d\ 3/2[7/2]_3$	72 977.4	10.901	10.	1.3×10^4
10	$6p15d\ 3/2[5/2]_2$	73 094.4	11.666	4.9	7.7×10^3
11	$6p15d\ 3/2[5/2]_3$	73 098.9	11.697	11.6	1.9×10^4
12	$6p15d\ 3/2[3/2]_1$	73 115.3	11.821	1.0	1.7×10^3
13	$6p15d\ 3/2[7/2]_3$	73 126.2	11.915	6.8	1.1×10^4
14	$6p16d\ 3/2[5/2]_3$	73 220.3	12.701	7.9	1.6×10^4
15	$6p16d\ 3/2[3/2]_1$	73 233.4	12.841	1.2	2.6×10^3
16	$6p16d\ 3/2[7/2]_3$	73 241.7	12.905	4.6	9.8×10^3
17	$6p17d\ 3/2[5/2]_3$	73 316.5	13.707	0.7	1.7×10^3
18	$6p17d\ 3/2[3/2]_1$	73 325.9	13.818	3.2	8.4×10^3
19	$6p17d\ 3/2[7/2]_3$	73 334.3	13.920	3.0	8.0×10^4
20	$6p18d\ 3/2[5/2]_3$	73 391.9	14.707	-	-
21	$6p18d\ 3/2[3/2]_1$	73 400.9	14.819	-	-
22	$6p18d\ 3/2[7/2]_3$	73 406.7	14.905	4.1	1.4×10^4

Table 1. Term energies and Γ (FWHM) cm^{-1} of $6p_{3/2}nd$ autoionizing Rydberg levels excited from the initial $6p5f\ 1/2[5/2]_2$ level.

Sr No	Assignments	Term energy (cm^{-1})	n^*	Γ (cm^{-1})	$\Gamma\ n^{*3}$
1	$6p5g\ 3/2[5/2]_2$	69 479.5	4.982	3.1	3.8×10^2
2	$6p5g\ 3/2[5/2]_3$	69 484.2	4.985	1.8	2.3×10^2
3	Unassigned	69 487.3	4.986	2.6	3.2×10^2
4	$6p5g\ 3/2[7/2]_3$	69 506.6	4.997	1.9	2.4×10^2
5	$6p15s\ 3/2[3/2]_2$	72 835.6	10.151	1.5	1.6×10^3
6	$6p15s\ 3/2[3/2]_1$	72 849.2	10.217	1.9	2.0×10^3
7	$6p11g\ 3/2[5/2]_{2,3}$	72 993.5	10.998	1.9	2.5×10^3
8	$6p16s\ 3/2[3/2]_2$	73 017.8	11.16	1.4	2.0×10^3
9	$6p16s\ 3/2[3/2]_1$	73 027.9	11.214	2.6	3.7×10^3
10	$6p12g\ 3/2[5/2]_{2,3}$	73 135.2	11.971	5.2	8.9×10^3
11	$6p17s\ 3/2[3/2]_1$	73 164.9	12.215	1.0	1.9×10^3
12	$6p13g\ 3/2[5/2]_{2,3}$	73 249.1	12.978	1.8	4.0×10^3
13	$6p18s\ 3/2[3/2]_1$	73 271.9	13.212	1.0	2.0×10^3
14	$6p14g\ 3/2[5/2]_{2,3}$	73 337.3	13.972	1.7	4.7×10^3
15	$6p19s\ 3/2[3/2]_2$	73 352.9	14.154	-	
16	$6p19s\ 3/2[3/2]_1$	73 357.3	14.212	-	
17	$6p15g\ 3/2[5/2]_{2,3}$	73 411.1	14.980	-	
18	$6p20s\ 3/2[3/2]_1$	73 426.7	15.216	-	

Table 2. Term energies and Γ(FWHM) cm^{-1} of $6p_{3/2}ns$, $6p_{3/2}ng$ autoionizing Rydberg levels excited from the initial $6p5f$ $1/2[5/2]_2$ level.

where $ip = 73\,900.65$ cm^{-1} and $R_{\rm Pb} = 109\,737.02$ cm^{-1} is the mass corrected Rydberg constant for lead and μ_ℓ is the quantum defect. The calculated effective quantum numbers and line widths Γ cm^{-1} of the $6p_{3/2}nd$ ($J = 1, 2, 3$) levels are also listed in Table 1.

In the present work we prepared the atomic beam of lead at higher temperature in order to raise the atomic density in the laser interaction region. The high atomic density also increases the atomic collisions and consequently enhances the line widths of the lines. The line widths of all the three dye lasers employed in the present work are about 0.3 cm^{-1} and the increased collision effects might have contributed to the widths of autoionizing levels of the order of $\approx$1 cm^{-1}.

The conspicuous absence of the $6pns\ 3/2[3/2]_2$ ($n \geq 15$) series, as remarked by Bhatti et al. [15], have been carefully examined in the present work. It is observed that the absence of the $6pns\ 3/2[3/2]_2$ series is not a regular phenomena. The strong noise background in the earlier work might have affected the corresponding region. We have been able to register these missing transitions. The term energies of all the observed $6p_{3/2}ng$ ($5, 11 \leq n \leq 15$) and $6pns\ 3/2[3/2]_{1,2}$ ($15 \leq n \leq 20$) levels along with the calculated effective quantum numbers and line widths (FWHM) $\Gamma(cm^{-1})$ are tabulated in Table 2.

In conclusion we have presented the spectrum of the odd parity $6p_{3/2}n\ell$ ($\ell = 0, 2, 4$ and $J = 1, 2, 3$) autoionizing Rydberg levels of lead, excited from the $6p5f\ 1/2[5/2]_2$ intermediate level. Term energies of about forty $6p_{3/2}ns$ ($J = 1, 2$), ($15 \leq n \leq 20$), $6p_{3/2}nd$ ($J = 1, 2, 3$), ($8, 13 \leq n \leq 18$) and $6p_{3/2}ng$ ($J = 2, 3$), ($5, 11 \leq n \leq 15$) levels are listed. Among these, six members of the $6p_{3/2}ng$ ($5, 13 \leq n \leq 15$) series and three new levels of the $6p_{3/2}8d$ configuration are observed for the first time. The $6p_{3/2}5g$ ($J = 2, 3$) is the lowest multiplet of $6p_{3/2}ng$ series which reveals the multiplet structure. The normalized line widths are also evaluated which signify the nonperturbation of the observed series.

We are grateful to the Pakistan Science Foundation (PSF), Pakistan Atomic Energy Commission (PAEC), ICTP Trieste, Italy and the Quaid-I-AzamUniversity for the financial assistance.

References

1. W.R.S. Garton, M. Wilson, Proc. Phys. Soc. **87**, 841 (1966)
2. R.D. Wood, K.L. Andrew, J. Opt. Soc. Am. **58**, 818 (1968)
3. C.M. Moore, *Atomic Energy Levels NSRDS-NBS* (US Govt Printing Office, Washington, DC, 1991)
4. C.M. Brown, S.G. Tilford, M.I. Ginter, J. Opt. Soc. Am. **67**, 1240 (1977)
5. J.P. Connerade, W.R.S. Garton, M.W.D. Mansfield, M.A.P. Martin, Proc. R. Soc. A **357**, 499 (1977)
6. M.A. Bolshov, A.V. Zybin, V.G. Koloshinkov, K.N. Koshelev, Spectroch. Acta B **32**, 279 (1977)
7. P. Buch, J. Nellessen, W. Ertmer, Phys. Scr. **38**, 664 (1988)
8. W.A. Young, M.Y. Mirza, W.W. Duley, J. Phys. B: At. Mol. Phys. **13**, 3175 (1980)
9. D.J. Ding, M.X. Jin, H. Liu, X.W. Liu, J. Phys. B: At. Mol. Phys. **22**, 1979 (1989)
10. J. Dembezynski, E. Stachowska, M. Wilson, P. Bush, W. Ertmer, Phys. Rev. A **49**, 745 (1994)
11. S. Farooqi, M. Nawaz, S.A. Bhatti, N. Ahmad, M.A. Baig, J. Phys. B: At. Mol. Opt. Phys. **28**, 2875 (1995)
12. S. Hasegava, A. Suzuki, Phys. Rev. A **53**, 3014 (1996)
13. S.A. Bhatti, M. Nawaz, S.M. Farooqi, A. Ahad, Saira Butt, N. Ahmad, M.A. Baig, J. Phys. B: At. Mol. Opt. Phys. **30**, 1179 (1997)
14. M. Nawaz, S.M. Farooqi, S.A. Bhatti, A. Ahad, Saira Butt, N. Ahmad, M.A. Baig, J. Phys. B: At. Mol. Opt. Phys. **30**, 3107 (1997)
15. S.A. Bhatti, M. Nawaz, S.M. Farooqi, A. Ahad, Saira Butt, N. Ahmad, M.A. Baig, J. Phys. B: At. Mol. Opt. Phys. **30**, 4183 (1997)
16. W. Hansch, Appl. Opt. **11**, 895 (1972)
17. C. Hanna, P.A. Karkkainnen, R. Wyatt, Opt. Quant. Electron. **7**, 115 (1975)